International Journal of Nanoelectronics and Materials
Volume 13, No. 4, Oct 2020 [671-686]

Optical and Morphological Properties of SiO_2-PVA and Er^{3+}-doped SiO_2-PVA Thin Film and Nanofibers

Nurul Iznie Razaki[1], Suraya Ahmad Kamil[1*] and Mohd Kamil Abd Rahman[1]

[1]*Faculty of Applied Sciences, Universiti Teknologi MARA, 40450 Shah Alam, Selangor, Malaysia.*

Received 1 June 2020, Revised 30 September 2020, Accepted 31 October 2020

ABSTRACT

SiO_2-PVA and Er^{3+}-doped SiO_2-PVA solution have been successfully prepared via sol-gel method. The main solution was transparent indicating the homogeneous mixture of SiO_2 and PVA components. Thin film and nanofiber layer were fabricated using spin coating and electrospinning technique, respectively. Effect of the SiO_2: PVA weight ratio was investigated to control the optical properties of the sample as well as the fibers diameter and their morphological appearance. The average diameter of the fiber varied from 79.41 to 122.20 nm depends on the SiO_2: PVA weight ratio. It was found that electrospinning of the low viscosity of the solution leads to the formation of fiber with beads-on-string morphology. The weight ratio of SiO_2: PVA (1:9) provides adequate chain entanglement as it produced dense fiber collection with fewer defects. All the samples are fully transparent in the VIS and NIR region, as evidenced by the percentage of transmittance with the range from 76% to 88%. Photoluminescence study shows that Er^{3+}-doped SiO_2-PVA nanofibers exhibit maximum red emission intensity at 0.4 wt. % of Er^{3+} doping. Er^{3+} doping did not significantly affect the diameter of the nanofibers due to relatively low concentration.

Keywords: Nanofiber, Er^{3+}-Doped, Optical Materials, Rare-Earth, Electrospinning.

1. INTRODUCTION

Hybrid inorganic-organic materials are of interest as it combines excellent properties of the organic part such as lightweight, processability and flexibility whereas the inorganic part is responsible for the good chemical stability with strong mechanical strength, which is ideal for a wide variety of applications [1-2]. Silica (SiO_2)-based is a promising material due to its high quality, strong thermal resistance, good chemical stability and highly transparent in the UV-VIS-NIR range [3-4]. Meanwhile, poly (vinyl alcohol) (PVA) polymer is an inexpensive and non-toxic material with good chemical and physical properties such as chemical resistance, water solubility and high melting point. Furthermore, a water-soluble polymer reacts with several cross-linking agents to form a gel. Incorporation of SiO_2-PVA as a nanocomposite would offer improved and unique properties, thus open up new possibilities in numerous applications [5-6]. It is reported that the mixture of SiO_2-PVA material demonstrated high transparency, thermostability and mechanical strength [7]. Incorporation of rare-earth (RE) ions in the hybrid inorganic-organic system are beneficial for luminescence properties of the materials as the ions have a wide range of emission lines from the ultra-violet to near infra-red spectral range [8-10]. Er^{3+} is one the RE elements that attracted considerable attention in numerous applications (i.e. laser, lighting and optical amplifier) due to its emission in the blue, red, green and near-infrared spectral range [11-13].

*Corresponding Author: *suraya_ak@uitm.edu.my*

Sol-gel provides a synthetic pathway for the incorporation of organic and inorganic materials. The sol-gel technique is a low-temperature route with the flexibility of composition and structure [14-16]. This method allows one to produce thin film or fibers directly from the solution. For the hybrid case, the properties of hybrid sol-gel derived materials can be tailored by varying the composition at its micro or nanostructure [17].

One-dimensional nanostructures such as nanofiber, nanowire, nanoparticles, etc. have attracted considerable attention due to their outstanding properties such as nano-sized, lightweight, high porosity and large surface area to volume ratio [18-19]. Nanofibers have been extensively studied for various applications including sensors, catalyst, display, laser, etc. [20-22] and it can be fabricated by a various technique including drawing, porous template, electrospinning and self-assembly [23]. Electrospinning is a simple procedure which draws very fine fibers from a viscous liquid (usually a polymeric solution) under the force of an electrostatic field. The electrospinning solution requires a concentration high enough to provide entanglements with viscosity low enough to allow motion induced by the electric field. Due to that, viscosity is one of the key parameters that affect the properties of the electrospun nanofibers. Usually, the polymer is added into a less viscous solution (inorganic) to increase the viscosity as well as the polymer entanglement of the solution [24-26]. Combination of the sol-gel and electrospinning techniques allows one to fabricate the fibers with tailorable morphology, diameter and composition [27-28].

In this work, we report on the preparation and characterization of the SiO_2-PVA and Er^{3+}-doped SiO_2-PVA in the form of thin film and nanofiber. Effect of the weight ratio of SiO_2: PVA and Er^{3+}-doping on the optical properties of the thin film sample were studied. Surface morphology and fiber diameter of these electrospun materials were also examined.

2. MATERIALS AND METHODS

2.1 Materials

Tetraethylorthosilicate, TEOS ($Si(OC_2H_5)_4$, MW=208.33, poly (vinyl alcohol), (PVA, MW=205,000) and erbium chloride hexahydrate ($ErCl_3.6H_2O$) and hydrochloric acid, HCl (MW= 36.47) were purchased from Sigma Aldrich. Ethanol, EtOH (C_2H_5OH), MW=46.07) was supplied from Kollin Chemicals. Ultra-pure water, H_2O (MW: 16), was also used in the preparation of the sol-gel solution.

2.2 Preparation of SiO_2-PVA and Er^{3+}-Doped SiO_2-PVA Solution

Polymeric PVA solution (7 wt. %) was prepared by dissolving the PVA powder with H_2O. The solution was then stirred vigorously using magnetic stirrer (Torrey Pines Scientific HS40-2) at the constant speed of 500 rpm at 60°C. SiO_2 active solution was obtained by mixing TEOS, H_2O, HCl and EtOH with the molar ratio of 1: 0.01: 2: 37.9 (TEOS: HCl: H_2O: EtOH). This ratio was chosen as it demonstrated dense, homogeneous and transparent SiO_2-based thin film [29]. This solution was stirred for one hour at 65°C under vigorous stirring of 400 rpm. In order to reveal the effect of the PVA concentration, hybrid SiO_2-PVA solution was prepared by mixing the polymeric PVA and SiO_2 solution with six different weight ratio as presented in Table 1. Er^{3+} ion solution was prepared by dissolving a small amount of $ErCl_3.6H_2O$ salt with a few drops of ultra-pure H_2O (e.g. 0.12 g for 0.6 wt.% of Er^{3+}). The solution was manually stirred using a glass rod to ensure the dopant was completely dissolved. Then, the diluted Er^{3+} ion solution was introduced in the hybrid SiO_2-PVA as $ErCl_3.6H_2O$ aqueous solution. The resultant mixture was stirred at the speed of 400 rpm at room temperature for 16 hours.

Table 1 Sample ID according to their respective SiO_2 and PVA weight ratio in a SiO_2-PVA mixture solution

No.	Sample ID	PVA (wt. %)	SiO_2 (wt.%)
1	PVA	100	0
2	SiO_2	0	100
3	S1P9	90	10
4	S2P8	80	20
5	S3P7	70	30
6	S4P6	60	40
7	S5P5	50	50
8	S6P4	40	60

2.3 Preparation of Thin Film and Nanofiber

The thin film of SiO_2-PVA and Er^{3+}-doped SiO_2-PVA were deposited on the substrate using a spin coater, with the spinning speed of 2000 rpm for 10 seconds. For the nanofiber deposition, the spinnable solution is filled into the 10 mL syringe with a metal needle that was mounted on a programmable syringe pump which controls the feeding rate of the solution. During the electrospinning process, a positive 12 kV voltage was applied to the rotating metal collector, covered with aluminium foil. The distance between the needle tip and the collector was fixed at 10 cm. The flow rate of the electrospinning solution was 0.5 mL/h. The sample was then heated at 80°C for 10 minutes to dry the sample.

2.4 Sample characterizations

The viscosity of the solution was measured using Viscometer (Brookfield). Glass transition temperature of the sample was determined using Differential Scanning Calorimetry (DSC) (NETZSCH, DSC 200 F3) under nitrogen environment. A sample weighing between of 10 – 12 mg was scanned at a heating rate of 10°C/min from 10°C to 100°C. The optical transparency of the fabricated sample in 200 -2000 nm range was acquired by Cary 5000 (1.12 Version) UV-VIS-NIR Spectrophotometer (Perkin Elmer), at room temperature. Deuterium lamp was used as a light source to illuminate the sample and the scanned rate was 600 nm/min. Refractive index and thickness of the thin film was measured by prism coupler (SAIRON SPA 4000-R) using 632.8 nm laser source, based on m-lines technique. The measurement was performed by using Gadolinium Gallium Garnet (GGG) prism. Presence of electrospun nanofiber with their morphology was analyzed by field emission scanning electron microscopy (FESEM) imaging (SUPRA40VP). Energy disperse x-ray (EDX) mapping was employed to perform elemental analyses of the sample. Before the imaging, the sample was sputter coated with gold to create a conductive surface. An average fiber diameter was analyzed using ImageJ software (NIH, USA) by measuring the diameter of at least 15 single fibers. Emission characteristics of Er^{3+} ions in visible range was carried out by Horiba Jobin Yvon Spectrophotometer. The measurement was performed at room temperature, upon 514.5 nm excitation of Argon laser.

3. RESULTS AND DISCUSSION

3.1 Effect of SiO_2: PVA Weight Ratio on the Optical and Morphological Properties of Hybrid SiO_2-PVA Thin Film and Nanofiber

Figure 1 showed the physical appearance of the fabricated thin film on the substrate. All samples exhibit similar appearance which is colorless and transparent, suggesting good compatibility of PVA and SiO_2 on a nanoscopic scale [7].

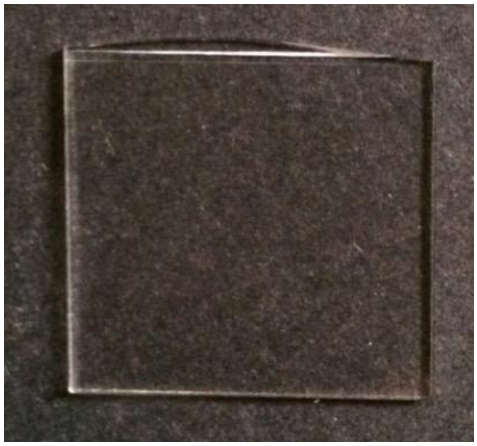

Figure 1. Fabricated thin film of sample S4P6.

Glass transition temperature, T_g of PVA and its hybrid (S1P9 and S7P3) is provided in Table 2. It is shown that pure PVA sample exhibited T_g at 64°C. It is expected that incorporation of SiO_2 to the PVA increased the glass transition of the hybrid. However, the T_g of the PVA-SiO_2 sample is found to be slightly lower than pure PVA. Based on previous study, the presence of SiO_2 has reduced the onset temperature of PVA, which is believed due to disruption in intermolecular interactions in the PVA [31].

Table 2 Glass transition temperature, T_g of PVA and its hybrid sample

Sample	Glass transition temperature, (T_g) (°C)
PVA	64.0
S1P9	63.5
S7P3	56.2

Degree of transparency of SiO_2 and SiO_2-PVA film samples as a function of incident wavelength was studied in the range of 200-2000 nm, as shown in Figure 2. All the samples are fully transparent in the VIS and NIR region, as evidenced by the percentage of transmittance with the range from 76% to 88%.

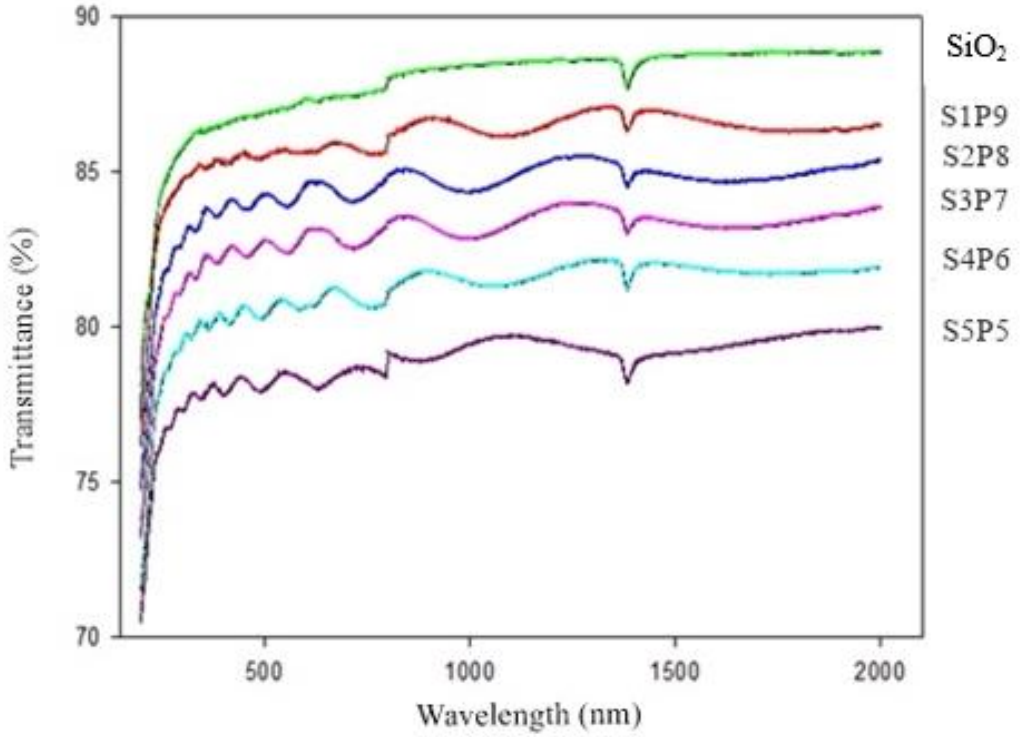

Figure 2. Transmittance spectra of SiO_2 and hybrid SiO_2-PVA samples, acquired in the UV-VIS-NIR wavelength range.

It is seen that the transparency of the samples increases with the increment of the wavelength with a similar pattern of the spectrum. Pure SiO_2 sample demonstrates the highest transmittance transparency, which is around (86-88%). The transparency is reduced with the incorporation of the PVA component in the SiO_2 matrix. Uniform ripples found in the transmission spectra of the S2P8 and S3P7 sample indicates uniform and smooth surface of the thin film. Interference effects give rise to the transmittance spectrum with successive maxima and minima indicating the uniformity of the film thickness [32-33]. In general, transmission measurement involves with the characterization of the optical behavior of the sample as a function of wavelength by comparing the intensity of light a sample (I) to the intensity of light before it passes over the sample (I_o). Appearance of the irregular ripples in the transmittance spectrum of the SiO_2, S1P9, S4P6 and different curve pattern of the S5P5 samples might be attributed to rough surface or presence of small particles on the top of the film during measurement. Presence of a small drop at the wavelength range of 1350 nm to 1400 nm is believed due to the intermolecular interaction between Si-O-Si linkages absorption vibration [34]. The Si-O-Si bonding is attributed to characteristics of SiO_2, confirming the presence of SiO_2 glass network. Furthermore, the presence of Si-O-Si bonding indicates that incorporating PVA to the inorganic precursor does not interrupt formation of SiO_2 network in the hybrids [31], as shown in Figure 3.

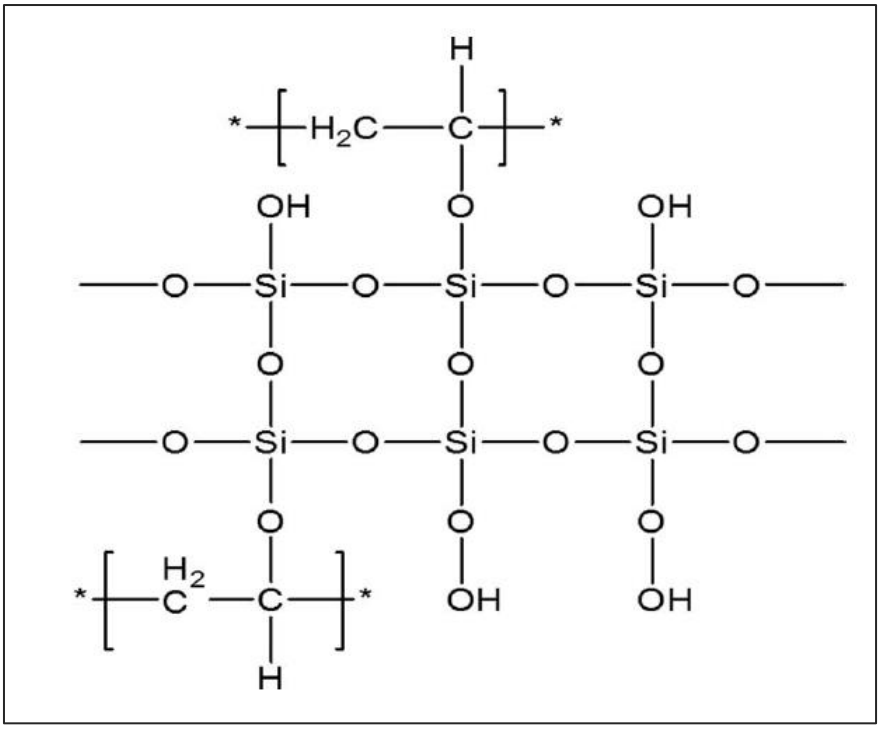

Figure 3. Schematic of SiO_2-PVA network structure [35].

For refractive index measurement, one pure PVA and two-hybrid SiO_2-PVA thin film samples (S4P6 and S6P4) were chosen for index comparison purpose. Table 3 shows the refractive index and thickness of the corresponding samples, measured with the prism coupler based on m-lines technique. It is observed that pure PVA film exhibits the highest refractive index, which is 1.56 and decreases with an increasing composition of SiO_2 in the hybrid matrix. Decreased in the refractive index could be attributed by low optical density as well as the packing density of the films [36].

Table 3 Refractive index and film thickness of the pure PVA and hybrid SiO_2-PVA sample

No.	Sample ID	Refractive index, n	Film thickness, µm
1	PVA	1.56	3.21
2	S4P6	1.52	3.49
3	S6P4	1.48	3.08

Figure 4 (a) depicts the FESEM image of the pure PVA (7 wt. %) fibers. The as-spun fibers were homogeneously dispersed with an average diameter of 238.25 ± 48.28 nm. The fibers were randomly oriented and they demonstrate smooth morphology without any appearance of beads on the fiber string. The sample is also free from any contaminations or impurities as, as confirmed by EDX spectrum (Figure 4(b)).

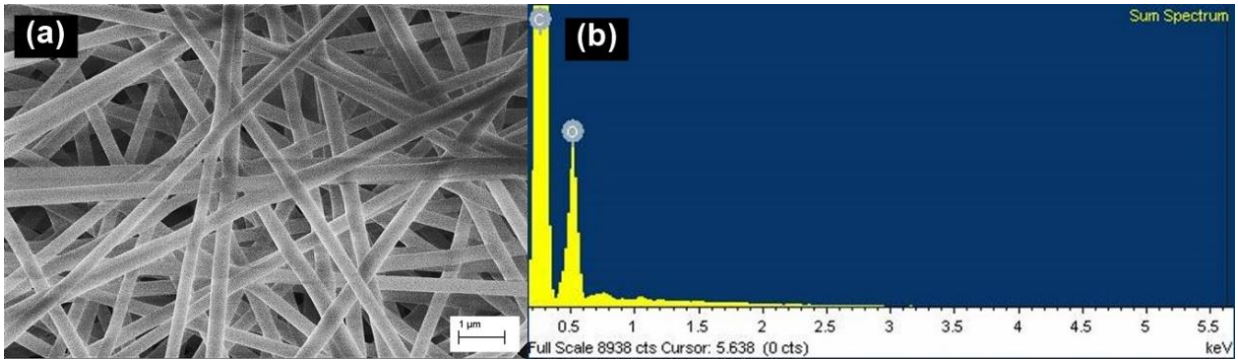

Figure 4. (a) FESEM images of the electrospun fiber of pure PVA (7 wt.%), scanned at the magnification of 10.00 K X and (b) EDX mapping of the sample showing the presence of Carbon (C) and Oxygen (O) elements.

Figure 5 shows the FESEM image of the as-spun hybrid SiO_2-PVA fibers with six weight ratios of SiO_2: PVA. The collected fibers were randomly oriented with length up to several centimeters long. Several thick fibers were observed due to merging of two or more thin fibers during the electrospinning process. It can be seen that as SiO_2 incorporated into the polymeric PVA solution, properties of the electrospun fibers such as morphology and diameter changed. The electrospun fibers of the S1P9 sample demonstrate uniform fiber size with minimal presence of beads on the fiber string. Meanwhile, a lot of beads with various shapes are observed in the S3P7, S4P6 and S5P5 electrospun fibers collection.

It is known that the viscosity of the electrospinning solution is one of the key parameters that affect the properties of the resultant electrospun fiber. The viscosity of the pure PVA and hybrid SiO_2: PVA solutions are shown in Table 4. It is expected that the viscosity of the solution is decreased as the fraction of SiO_2 is increased. This phenomenon could be explained by an enhancement of agglomeration of polysilica species in the concentrated silica sol [37-38]. At this proportion range, it is believed that cross-linking between the PVA and SiO_2 during the preparation process is responsible for the increase in viscosity of the hybrid solution. As reported by Pirzada et al., the increase cannot be attributed to the SiO_2 network only, since TEOS alone does not demonstrate such a high viscosity. Thus, it is possible that cross-linking of PVA by the silanol groups caused an increase in the viscosity of the solution due to higher effective molecular weight [31]. However, for the S2P8 solution, the viscosity is increased drastically from 264 cPs to 433 cPs. Furthermore, this solution tends to transform to gel within 2 hours to one-day period. This abnormal condition is found at this weight ratio and the solution is cloudy when compared to S1P9. It is believed that the strong attractive interaction between particles at a particular concentration result in the highest agglomeration for sample S2P8.

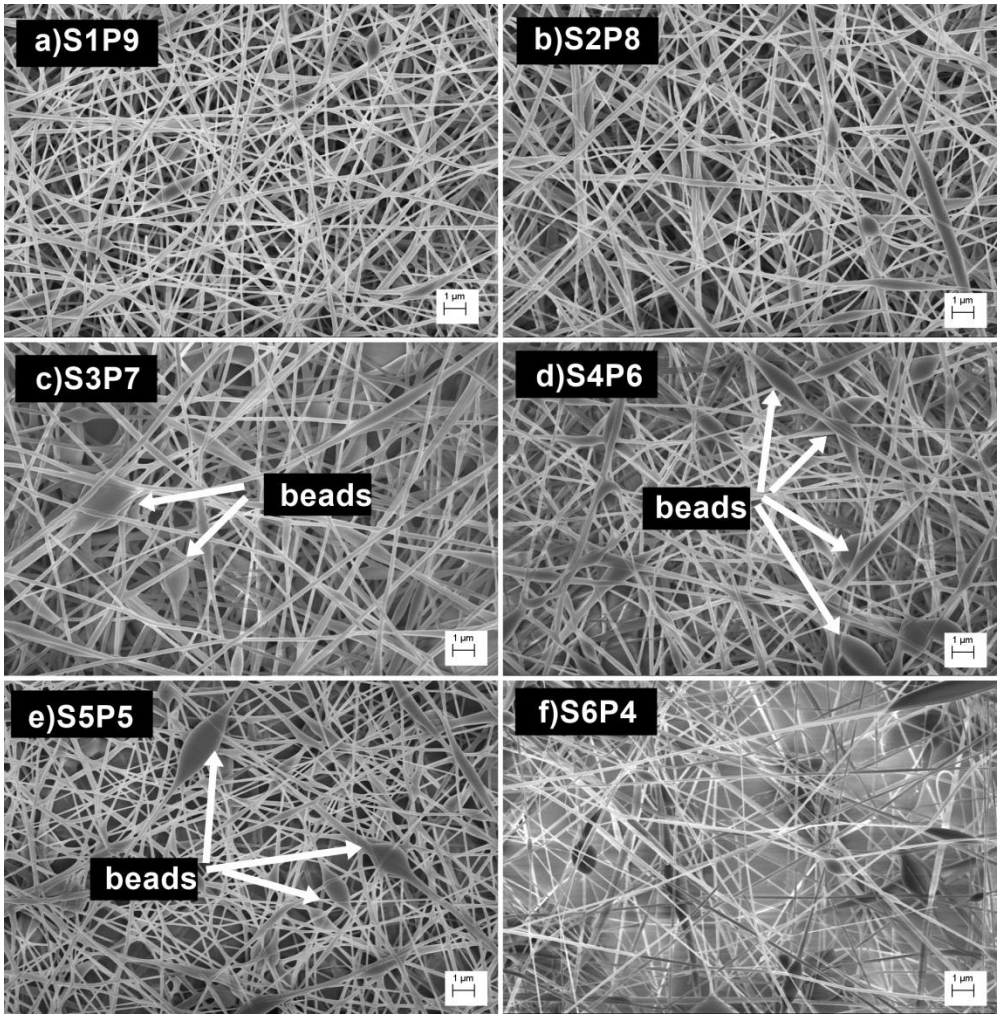

Figure 5. FESEM image of the as-spun fiber of (a) S1P9 (b) S2P8 (c) S3P7 (d) S4P6 (e) S5P5 and (f) S6P4, scanned at the magnification of 5 K X. Arrows show formation of beads on the fiber string.

Table 4 Viscosity of pure PVA and hybrid SiO_2-PVA solution with their average diameter of the electrospun fiber

No.	Samples Nomenclature	Viscosity (cPs)	Average diameter of the fiber (nm)
1	S1P9	264	122.20 ± 47.63
2	S2P8	433	143.74 ± 49.14
3	S3P7	155	108.34 ± 45.42
4	S4P6	105	82.90 ± 26.51
5	S5P5	60	100.85 ± 32.05
6	S6P4	31	79.41 ± 33.05

In general, an increment of the viscosity of the electrospinning solution resulted in higher entanglements of the polymer chain which then produced thicker fiber. This is attributed to the high resistance of the stretched polymeric solution during the electrospinning process [19], [24]. In this study, as shown in Table 4, the average diameter of the hybrid SiO_2-PVA nanofibers decreased with the increment of SiO_2 component in the matrix, except for the sample of S2P8 and S5P5. The diameter of the electrospun fiber ranges from 79.41±33.05 nm at low viscosity (31cPs) to 143.74±49.14 nm at higher viscosity (433cPs). S2P8 sample demonstrates thicker fiber due to the high viscosity of the solution. As for S5P5 sample, the average diameter of the fiber is slightly increased due to the presence of thick fibers and large beads on the fiber string. The formation of beaded fibers from the solutions with lower viscosity could be attributed to a breakup of the jet

while travelling in the air by surface tension [39]. It is reported that the formation of beads whose size is bigger than fiber can lead to low mechanical properties of the fibers [40-41]. Furthermore, it is observed that the collected fibers of the low viscosity of the solution demonstrate large variation in fiber diameter. This is believed due to bending instability associated with the electrified spinning jet, that caused an unstable jet trajectory towards the metal collector during the electrospinning process [19], [24]. Besides that, ambient conditions during the electrospinning process such as humidity and temperature of the laboratory could also be the contribution to the inconsistency of fiber diameter.

Based on the presented results, it can be concluded that 1:9 ratio of hybrid SiO_2: PVA provides smooth morphology of the electrospun fibers with dense fiber distribution and minimal beads formation. Furthermore, the sample exhibit high transparency that is beneficial for optical application. For this reason, it was decided to use this ratio to continue with the experimental work on the effect of Er^{3+} doping on the properties of the hybrid SiO_2: PVA nanocomposite.

3.2 Effect of Er^{3+} Doping on the Optical and Morphological Properties of SiO_2-PVA Thin Film and Nanofiber

In order to study the effect of RE dopant, the various concentration of $ErCl_3.6H_2O$ aqueous solution was added into the hybrid SiO_2-PVA (S1P9) solution, as previously described. This proportion of SiO_2:PVA was chosen because it provides adequate chain entanglement as evidenced by uniform fiber dispersion with less formation of beads on fiber string. Generally, a polymer material that has a $T_g \leq$ room temperature is not feasible to be used as in several photonics application since at that temperature, it will develop some sort of "rubbery" effect which in turn will affect its performance. In this study, T_g measurement of the sample is carried out to ensure the compatibility of the RE-doped SiO_2-PVA in optical application as the dopant could alter the optical properties of the material. Table 5 shows the glass transition temperature (T_g) for three different concentrations of Er^{3+} (0.2 wt. %, 0.4 wt. % and 0.6 wt. %) with fixed ratio of SiO_2: PVA (1:9). It can be seen that by varying the Er^{3+} doping from 0,2 to 0.6 wt.%, the T_g of the sample showed insignificant change in the value. As the T_g is above 60°C, which is higher than the room temperature, it can be conclude that at this doping range, this material is a good candidate for photonics application.

Table 5 Glass transition temperature of the hybrid SiO_2-PVA (S1P9) sample with different Er^{3+} doping concentration

Er^{3+} doping in (SiO_2: PVA) (1:9) (wt. %)	Glass transition temperature, (T_g) (°C)
0.2	62.5
0.4	63.7
0.6	63.5

Transmission spectra of Er^{3+}-doped SiO_2-PVA samples are shown in Figure 6. The transmission spectra reveal that the thin film demonstrates high transparency in the UV-VIS-NIR wavelength range. Sample with 0.2% and 0.6% of Er^{3+} doping shows high transmittance spectra (~85%) and slightly dropped to 78% for the sample having 0.4% of Er^{3+}. This might be due to thicker film formation during the spin coating process that leads to lower transparency.

Emission characteristic of the hybrid SiO_2-PVA doped with various Er^{3+} concentration is studied. As seen in Figure 7, all the samples demonstrate red emission line which assigned to $^4F_{9/2} \rightarrow {}^4I_{15/2}$ Er^{3+} ion transitions [42-43]. As the Er^{3+} ion concentration increases from 0.2% to 0.4%, the emission intensity also increase. However, when the concentration is further increased to 0.6%, the intensity is decreased and slightly shifted to lower energy. This is due to the nature of the RE dopant itself which tend to precipitate above certain dopant concentration, which will consequently lead to the formation of optically inactive Er^{3+} ions clusters. As a result, the

clustered ions interact and transfer the energy among each other, thus decrease the luminescence efficiency via cross-relaxation [13].

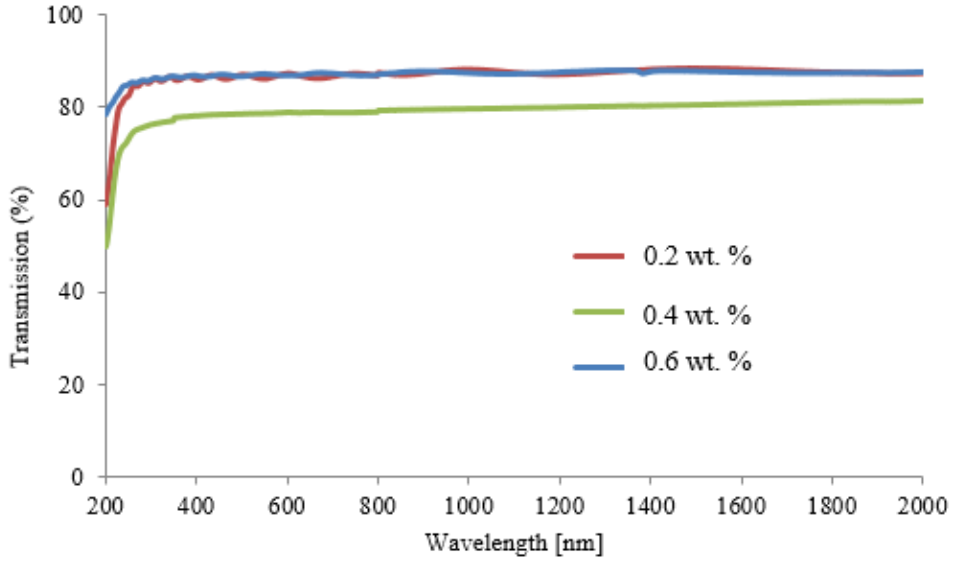

Figure 6. Transmission spectra of the hybrid SiO_2-PVA (S1P9) doped with various Er^{3+} concentration in the UV-VIS-NIR range.

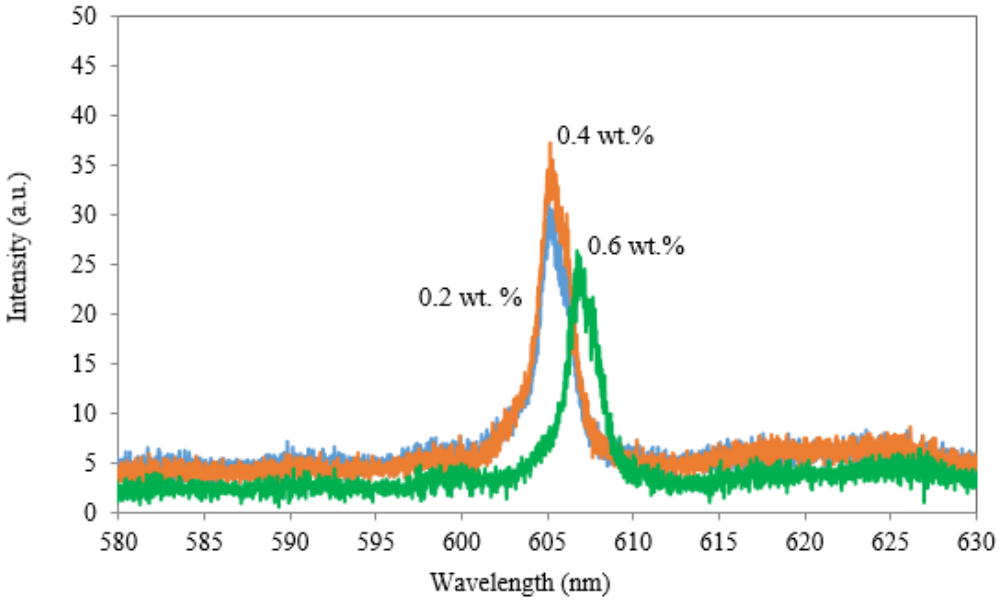

Figure 7. Red emission spectra of the hybrid SiO_2-PVA (S1P9) doped with various concentration of Er^{3+} under 514.5 nm excitation.

FESEM images of the Er^{3+}-doped SiO_2-PVA (S1P9) electrospun nanofiber is shown in Figure 8 (a1-c1). It is observed that the deposited fibers were cross-linked and randomly oriented on the substrate. The electrospun hybrid fiber with 0.2 wt. % of Er^{3+} demonstrates straight fibers with the formation of some beads on the string. At 0.4 wt. % doping, the deposited fibers show non-uniform fiber diameter distribution and presence of some curl fiber is observed. For the sample with 0.6 wt. % (Er^{3+}), the fiber diameter is obviously not uniform along each of the strands where there is high tendency to "bulge" and the distribution of the medium sizes and large sizes fiber seems to be equally likely to occur. The degree of entanglements is also higher for this concentration. The hybrid SiO_2-

PVA (S1P9) fibers doped with 0.2 wt. %, 0.4 wt. % and 0.6 wt.% of Er^{3+} exhibited average diameter of 122.95 ± 34.84 nm, 126.51 ± 25.94 nm and 129.0 ± 25.89 nm, respectively. It is observed that as the Er^{3+} concentration in the hybrid SiO_2-PVA is increased, there is a slight increase in the diameter of the fiber. Er^{3+} doping did not significantly affect the diameter of the hybrid fibers due to relatively low concentration.

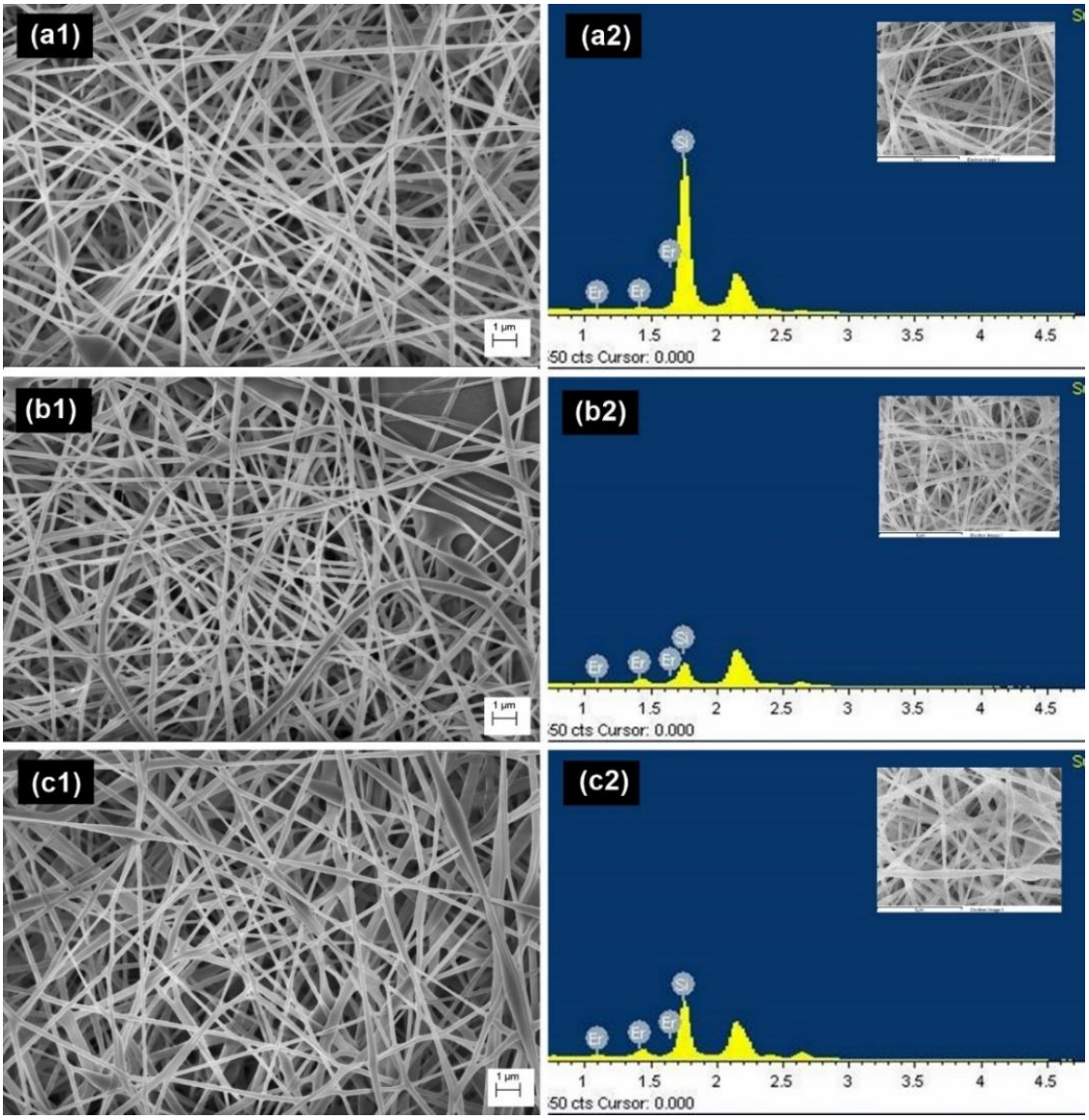

Figure 8. FESEM Images of the hybrid SiO_2-PVA Nanofiber doped with various Er^{3+} concentration (a1) 0.2 (b1) 0.4 and (c1) 0.6 (wt. %). EDX spectrum of the 0.2, 0.4 and 0.6 wt. % doped SiO_2-PVA sample is depicted by (a2), (b2) and (c2), respectively. The scanned area is presented by the inset image.

EDX spectrum of the samples (Figure 8 (a2-c2)) reveals the elemental composition within an area of the scanned nanofiber. Table 5 shows the fraction of each element in the hybrid Er^{3+}-doped SiO_2-PVA (S1P9) nanofiber. It is confirmed that the resulting nanofiber contains the preferred elements of C, O, Si and Er that produce Er^{3+}- doped SiO_2-PVA nanofiber.

Table 6 Elemental composition of Er^{3+}-doped SiO_2-PVA (S1P9) nanofibers

	Atomic %		
Element	**0.2% of Er^{3+}**	**0.4% of Er^{3+}**	**0.6% of Er^{3+}**
C K	73.44	76.25	74.67
O K	12.86	19.61	17.34
Si K	13.45	3.34	7.06
Er M	0.25	0.79	0.93
Total	100.00	100.00	100.00

From Table 6, it can be seen that carbon (C) element takes on a major proportion of the overall composition of the hybrid nanofiber. This is expected since the C group which came from the PVA $[(C_2H_4O)_x]$, is indeed the host for the overall solution with the ratio of 1:9 (SiO_2: PVA). In the case of Er^{3+} element, the least percentage of contribution of the element among others because the dopant added in the sample was very small in quantity. The fact that the small amount of Er^{3+} is detectable in the fiber strands indicates the compatibility of the resulting materials in producing a spinnable solution. On the other hand, Si element that supposed to be in minor quantity since the SiO_2 solution mixture ratio is 1, ended up having an atomic percentage larger than expected. This is because the Si atomic % may not be contributed solely by electrospun fibers, but also the substrate on which the fiber is deposited. In EDX, the electron bombardment caused the layers of deposited fibers to be cracked; thereby exposing the silicon substrate underneath and those interactions will contribute in percentage amount of Si in EDX spectra.

4. CONCLUSION

In summary, this work describes the preparation and characterization of the hybrid SiO_2-PVA and Er^{3+}-doped SiO_2-PVA materials by the sol-gel technique. Electrospinning of the hybrid solution with lower viscosity caused a formation of fibers with bead-on-string morphology. The optimum weight ratio of SiO_2: PVA for the electrospinning process was identified as 1:9 as it exhibited good spinnability. Small dopants concentration may not have a major influence on the overall size of the fiber but the tendency of the dopants to cluster at higher concentration may cause the bulging effect on some of the strands. The decrement of the red emission of Er^{3+} ions at 0.6 wt. % doping is likely a result of the ion clustering effect.

ACKNOWLEDGEMENTS

The project was financially supported by the Ministry of Education of Malaysia and Research Management Centre (RMC), Universiti Teknologi MARA through the FRGS grant [No. 600-IRMI/FRGS 5/3 (431/2019)].

REFERENCES

[1] T. E. Newsome & S. V. Olesik, "Electrospinning Silica/Polyvinylpyrrolidone Composite Nanofibers," Journal of Applied Polymer Science **131**, 21 (2014) 40966.
[2] V. P. Ananikov, "Organic-Inorganic Hybrid Nanomaterials," Nanomaterials. **9** (2019) 1197.
[3] Y. Qiao, N. Da, D. Chen, Q. Zhou, J. Qiu, & T. Akai, "Spectroscopic Properties of Neodymium Doped High Silica Glass and Aluminium Cooping: Effects on the Enhancement of Fluorescence Emission," Applied Physics B **87**, 4 (2007) 717-722.
[4] M. Hasanuzzaman, A. Rafferty, M. Sajjia & A.G. Olabi, "Properties of Glass Materials," Reference Module in Materials Science and Materials Engineering Elsevier (2015).

[5] K. Sasipriya, R. Suriyaprabha, P. Prabu & V. Rajendran, "Synthesis and Characterization of Polymeric Nanofibers Poly (Vinyl Alcohol) and Poly (Vinyl Alcohol)/Silica using Indigenous Electrospinning Set Up," Materials Research **16**, 4 (2013) 824-830.
[6] M. Yanilmaz, "Evaluation of Electrospun PVA/SiO_2 Nanofiber Separator Membranes for Lithium-Ion Batteries," The Journal of The Textile Institute **111**, 3 (2020) 447-452.
[7] H. Pingan, J. Mengjun, Z. Yanyan & H. Ling, "A Silica/PVA Adhesive Hybrid Material with High Transparency, Thermostability and Mechanical Strength," RSC Advances **7** (2016) 2450–2459.
[8] N. Pinna & M. Karmaoui, "Photoluminescent rare-earth based lamellar organic-inorganic hybrid nanoparticles" in Advanced Wet-Chemical Synthetic Approaches to Inorganic Nanostructures, P. D. Cozzoli, Ed. Kerala, India: Transworld Research Network, (2008) 391-406.
[9] S. Gao, P. Kuan, X. Li, L. Wang, M. Liao & L Hu, "Tm^{3+}-Doped Tellurium Germinate Glass and Its Double-Cladding Fiber for 2μm Laser," Materials Letters **143** (2015) 60-62.
[10] J. Liu, A. M. Kaczmarek & R. V. Deun, "Advances in Tailoring Luminescent Rare-Earth Mixed Inorganic Materials," Chemical Sociecty Reviews **47** (2018) 7225-7238.
[11] P. Rajanikanth, Y. Gandhi & N. Veeraiah, "Enrichment of Orange Emission of Er^{3+} Ion with Sn^{4+} Ion as Sensitizer in Lithium Lead Phosphate Glass System," Optical Materials **48** (2015) pp. 51-58.
[12] H. Aboud, "Enhanced Luminescence of Er^{3+}-Doped Zinc-Lead-Phosphate Glass Embedded SnO_2 Nanoparticles," Journal of Nanostructures **6**, 3 (2016) pp. 179-183.
[13] S. K. Taherunnisa, D. V. Krishna Reddy, T. Sambasiva Rao, K. S. Rudramamba, Y. A. Zhydachevskyy, A. Suchocki., M. Piasecki & M. Rami Reddy, "Effect of Up-Conversion Luminescence in Er^{3+} Doped Phosphate Glasses for Developing Erbium-Doped Fibre Amplifiers (EDFA) and G-LED's," Optical Materials X **3** (2019) 100034.
[14] J. Wang, Q. Ran, X. Xu, B. Zhu & W. Zhang, "Preparation and Optical Properties of TiO_2-SiO_2 Thin Films by Sol-Gel Dipping Method," IOP Conference Series: Earth and Environmental Science **310**, 44 (2019) 042029.
[15] S. M. Ashrafi-Shahri, F. Ravari & D. Seifzadeh, "Smart Organic/Inorganic Sol-Gel Nanocomposite Containing Functionalized Mesoporous Silica for Corrosion Protection," Progress in Organic Coatings **133** (2019) 44-54.
[16] S. Mura, R. Ludmerczki, L. Stagi, S. Garroni, C. M. Carbonaro, P. C. Ricci, M. F. Casula, L. Malfatti & P. Innocenzi, "Integrating Sol-Gel and Carbon Dots Chemistry for the Fabrication of Fluorescent Hybrid Organic-Inorganic Films," Scientific Reports **10**, 1 (2020) 1-12.
[17] M. Kamil Abd-Rahman & N. Iznie Razaki, "Effect of Nanofiber/Thin-Film Multilayers on the Optical Properties of Thulium-Doped Silica-Alumina," Journal of Luminescence **196** (2018) 442-448.
[18] B. Huang, C. Zhao, M. Zhang, Z. Zhang, E. Xie, J. Zhou. & W Han, "Doping Effect of In_2O_3 on Structural and Ethanol-Sensing Characteristics of ZnO Nanotubes Fabricated by Electrospinning," Applied Surface Science **349** (2015) 615-621.
[19] L. Persano, A. Camposeo & D. Pisignano, "Advancing the Science and Technology of Electrospinning and Functional Nanofibers," Macromolecular Materials and Engineering **32**, 8 (2017) 1700237.
[20] A. Gupta, D. V. Nandanwar & S. R. Dhakate, "Electrospun Self-Assembled Zno Nanofibers Structures for Photocatalytic Activity in Natural Solar Radiations to Degrade Acid Fuchsin Dye," Advanced Materials Letters **6**, 8 (2015) 706-710.
[21] M. A. Sobhan, A. Lebedev, L. L. Chng & F. Anariba, "Rapid Fabrication of Photoluminescent Electrospun Nanofibers Without the Need of Chemical Polymeric Backbone Modifications," Journal of Nanomaterials **2018** (2018) 1980357.
[22] X. Gao, S. Han, R. Zhang, G. Liu and J. Wu, "Progress in Electrospun Composite Nanofibers: Composition, Performance and Applications for Tissue Engineering," Journal of Materials Chemistry B **7** (2019) 7075-7089.

[23] I. Alghoraibi, & S Alomari, "Different Methods for Nanofiber Design and Fabrication," In Handbook of Nanofibers, A. Barhoum, M. Bechelany and A. Makhlouf, Eds. Springer Cham, (2018) 1-46.
[24] A. Haider, S. Haider & I-K. Kang, "A Comprehensive Review Summarizing the Effect of Electrospinning Parameters and Potential Applications of Nanofibers in Biomedical and Biotechnology" Arabian Journal of Chemistry **11**, 8 (2015) 1165-1188.
[25] T. J. Alwan, Z. A. Toma, M. A. Kudhier & K. M Ziadan, "Preparation and Characterization of the PVA Nanofibers Produced by Electrospinning" Madridge Journal of Nanotechnology & Nanoscience **1**, 1 (2016) 1-3.
[26] B.S. Chapman, S. R Mishra & J. B. Tracy, "Direct Electrospinning of Titania Nanofibers with Ethanol," Dalton Transactions **48** (2019) 12822-12827.
[27] E. Franco, R. Dussán, M. Amú & D. Navia, "Statistical Optimization of the Sol-Gel Electrospinning Process Conditions for Preparation of Polyamide 6/66 Nanofiber Bundles,"Nanoscale Research Letters **13** (2018) 230.
[28] M. T. Jafari, M. Saraji & M. Kermani, "Sol-Gel Electrospinning Preparation of Hybrid Carbon Silica Nanofibers for Extracting Organophosphorus Pesticides Prior to Analyzing Them by Gas Chromatography-Ion Mobility Spectrometry," Journal of Chromatography A **1558** (2018) 1-13.
[29] R. R. Goncalves, G. Carturan, L. Zampedri, M. Ferrari, M. Montagna, A. Chiasera, G. C. Righini, S. Pelli, S. J. L Ribeiro & Y. Messaddeq, "Sol-Gel Er-Doped SiO_2-HfO_2 Planar Waveguides: A Viable System for 1.5μm Application," Applied Physics Letters **81**,1 (2002) 28-30.
[30] K. Nakane,T. Yamashita, K. Iwakura & F. Suzuki, "Properties and Structure of Poly(Vinyl Alcohol)/Silica Composites," Journal of Applied Polymer Science **74** (1999) 133-138.
[31] T. Pirzada, S. A. Arvidson, C. D. Saquing, S. S. Shah & S. A. Khan, "Hybrid Silica-PVA Nanofibers via Sol-Gel Electrospinning,"Langmuir 28, 13 (2012) 5834-5844.
[32] N. M. Ahmed, Z. Sauli, U. Hashim and Y. Al-Douri, "Investigation of the Absorption Coefficient, Refractive Index, Energy Band Gap, & Film Thickness for $Al_{0.11}Ga_{0.89}N$, $Al_{0.03}Ga_{0.97}N$, and GaN by Optical Transmission Method," International Journal of Nanoelectronics and Materials **2,** 2 (2009) 189-195.
[33] H. Chen, A. Baitenov, Y. Li, E. Vasilena, S. Popov, I. Sychugov, M. Yan & L. Berglund, "Thickness Dependence of Optical Transmittance of Transparent Wood: Chemical Modification Effects," ACS Applied Materials & Interfaces **1** (2019) 35451-35457.
[34] A. Bandyopadhyay, M. De Sarkar & A. K. Bhowmick, "Poly (Vinyl Alcohol)/Silica Hybrid Nanocomposites by Sol-Gel Technique: Synthesis and Properties," Journal of Materials Science **40** (2005) 5233 – 5241.
[35] M. Dirican, M. Yanilmaz, K. Fu, O. Yildiz, H. Kizil, Y. Hu & X. Zhang, "Carbon-Confined PVA-Derived Silicon/Silica/Carbon Nanofiber Composites as Anode for Lithium-Ion Batteries," Journal of The Electrochemical Society 161, 14 (2014) 2197-2203.
[36] J. Wu, T-G. Qu, L-F. Gao, X-M. Yang, X-H. Li, Y-F.Tu & X-L. Zhu, "Special Odd-Even Effect of Oligomerization on Properties of Cyclic Olioesters," Chinese Journal of Polymer Science **33**, 8 (2015) 1069-1073.
[37] M. D. Sack & S. Sheu, "Rheological Properties of Silica Sol-Gel Materials," Journal of Non-Crystalline Solids **92** (1987) 383-396.
[38] S. Sakai, K. Kawakami & M. Taya, "Controlling Diameter of Silica Nano-Fibers Obtained from Sol-Gel/Electrospinning Methods," Journal of Chemical Engineering of Japan **45**, 6 (2012) 436-440.
[39] H. Zhao & H. Chi, "Electrospun Bead-On-String Fibers: Useless or Something of Value?" in Novel Aspects of Nanofibers, T. Lin, Ed. London, United Kingdom: Intech Open, (2018) 87-102.
[40] H. Fong, I. Chun & D.H. Reneker, "Beaded Nanofibers Formed During Electrospinning," Polymer **40**, 16 (1999) 4585 – 4592.
[41] J. M. Deitzel, J. Kleinmeyer, D Harris & N. C. Beck Tan, "The Effect of Processing Variables on the Morphology of Electrospun Nanofibers and Textiles," Polymer **42**, 1 (2001) 261-272.

[42] W. Ahn & Y. J. Kim, "Synthesis and Up-Conversion Luminescence of $Lu_3Al_5O_{12}:Yb^{3+}$, Er^{3+}," Optical Materials Express **6**, 4 (2016) 1099-1105.
[43] X. Shang, P. Chen, T. Jia, D. Feng, S. Zhang, Z. Sun & J. Qiu, "Upconversion Luminescence Mechanisms of Er^{3+} Ions under Excitation of an 800 nm Laser," Physical Chemistry Chemical Physics **17** (2015) 11481-11489.